Доклады Международной конференции "Математическая биология и биоинформатика". Под ред. В.Д. Лахно. Том 7. Пущино: ИМПБ РАН, 2018. Статья № e48. doi: 10.17537/icmbb18.83

Density functional study of magnetic substitutions in hydroxyapatite

Paramonova E.V.[1], Avakyan L.A.[2], Coutinho J.[3], Bystrov V.S.[1]

[1]*Institute of Mathematical Problems of Biology, Keldysh Institute of Applied Mathematics,RAS, Pushchino, Russia*
[2]*Physics Faculty, Southern Federal University, Rostov-on-Don, Russia*
[3]*Department of Physics and I3N, University of Aveiro, Aveiro, Portugal*

ekatp@yandex.ru

Hydroxyapatite is the major inorganic component of hard tissues of vertebrates. It is widely used in medicine as implant material due to its good biocompatibility. Introduction of magnetic defects into apatite structure is a perspective for medical applications in the field of hyperthermia anti-cancer treatment and magnetic resonance imaging diagnostics. In the current study the wide range of apatite structures with magnetic defects is investigated by density functional method. Defect structures of apatite including commonly considered substitutions of calcium in different crystallographic positions and series of iron interstitials were investigated. It is shown that interstitial iron in hydroxyl channel is the most probable. The substitutions of Ca(1) or Ca(2) by Fe have approximately equal probability of realization.

Key words: hydroxyapatite, defect engineering, magnetic materials, density functional modeling.

Исследование магнитных примесей в гидроксиапатите методами функционала плотности

Парамонова Е.В.[1], Авакян Л.А.[2], Коутиньо Ж.[3], Быстров В.С.[1]

[1]*Институт математических проблем биологии, Институт прикладной математики им. М.В. Келдыша РАН, Пущино, Россия*
[2]*Южный федеральный университет, Ростов-на-Дону, Россия*
[3]*Факультет физики и И3Н, Университет Авейру, Португалия*

Гидроксиапатит – основной минеральный компонент костной ткани, широко используется в медицине в качестве материала имплантов, благодаря хорошей биосовместимости. Внесение магнитных примесей в структуру гидроксиапатита является перспективным для применения в медицине для задач гипертермии и магнитно-резонансной диагностики. В работе проводится моделирование магнитных примесей структуры гидроксиапатита методами функционала плотности. Рассмотрен ряд дефектных структур, включающий в себя, как активно исследуемые дефекты замещения атомов кальция железом в различных кристаллографических позициях, так и дефекты внедрения, учитываемые впервые. Показано, что наиболее вероятна реализация дефекта типа внедрения в гидроксильном канале. Дефекты замещения железом в позиции Ca(1) и Ca(2) оказываются примерно равновероятными.

Ключевые слова: гидроксиапатит, проектирование дефектов, магнитные материалы, расчеты методами функционала плотности.

1. Introduction

Hydroxyapatite (HAP), $Ca_{10}(PO_4)_6(OH)_2$ is a bioceramic material with a calcium-to-phosphorus ratio similar to that of natural bone and teeth. There is therefore great clinical interest in its use, since it is biocompatible, bioactive and biodegradable. It is currently used for bone graft substitutes, such as porous granules, block scaffolds and coatings over metallic implants for bone regeneration. Particular physicochemical properties of the apatite structure allow it to form many different compositions, therefore allowing an easy incorporation of ions in the crystal lattice. Hydroxyapatite (HAP), $Ca_{10}(PO_4)_6(OH)_2$, which is the basic mineral component of hard tissues (bone,

***Proceedings of the International Conference "Mathematical Biology and Bioinformatics".** Ed. V.D. Lakhno. Vol. 7. Pushchino: IMPB RAS, 2018. Paper No. e48. doi: 10.17537/icmbb18.83*

teeth) has been extensively studied and used as a replacement material in medicine and dentistry. In addition to its application as a bioceramic material, it is proposed as an environmental adsorbent of metal ions due to its cation-exchange property.

The incorporation of impurites, via either ionic exchange or diffusion, affects morphology, solubility, lattice parameters, and consequently the stability of the material. The material, biological, and chemical properties are related with the variation in the electronic structure caused by defects and impurities. Thus it is necessary to understand the relationship between structural aspects and the material properties upon impurity incorporation [1, 2].

In recent years magnetic nanomaterials have received significant attention owing to their potential biomedical applications. Indeed magnetic particles have been progressively incorporated as support materials for enzyme immobilization, and have been used as drug-delivery agents, contrast agents for magnetic resonance imaging (MRI) as well as heat mediators for hyperthermia-based anti-cancer treatments and many other exciting biotechnological applications [3]. Due to the importance of having no-toxicity for the above-mentioned applications, the present work is focused on the investigation of a biocompatible and bioresorbable Fe-doped hydroxyapatite. This new magnetic apatite could represent, by virtue of its bioactivity, a conceptually new type of scaffold for hard tissue regeneration.

2. Hydroxyapatite structure

2.1. Pure hydroxyapatite structure

Hydroxyapatite has hexagonal structure with symmetry space group $P6_3/m$ and lattice parameters $a = b = 9.432$ Å, $c = 6.881$ Å. There is one formula unit $Ca_{10}(PO_4)_6(OH)_2$ (44 atoms) per unit cell (Fig. 1). The basic bonding and structural characteristics of ideal crystalline HAP show that there are two different calcium sites Ca(1) and Ca(2), as the target for cation substitution by metals. The phosphate tetrahedra PO_4 are linked by cations Ca, which are arranged on two nonequivalent sites. Ca^{2+} at the special site 4 f , denoted Ca(1), is sixfold coordinated to 3O(1) and 3O(2) atoms while Ca^{2+} at the site 6h, denoted Ca(2), is sixfold coordinated to 4O(3), O(2) and O_H atoms.

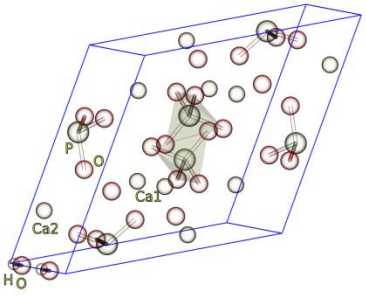

Fig. 1. The unit cell of pure HAP.

2.2. Iron substitutions

Iron impurities in HAp considered in literature are limited by Ca(1) and Ca(2) substitutions [1, 4, 5] illustrated on Fig. 2. In that studies the main attention is paid to the establishing of mechanism of ionic charge compensation, since due to their 3d electron configuration, Fe^{2+} and Fe^{3+} cations have flexible coordination geometries fourfold, fivefold, and sixfold in their compounds. For trivalent Fe^{3+} substitution at a Ca^{2+} site, Jiang et al [1] investigated the defected and nonstoichiometric case to consider charge compensation. At the Ca(1) site, a nonstoichiometric system $Ca_{10-x}(PO_4)_{6-x}(HPO_4)_x(OH)_2$, $x = 1$ was introduced, while another system $Ca_{10-x}(PO_4)_6(OH)_{2-x}$, $x = 1$ characterized by vacancies at hydroxyl and Ca(2) sites was considered for the Fe^{3+} substitution at Ca(2) sites.

In current study we will consider only single point defects and charge compensation will be accounted analyzing charged supercells, as it was performed in our recent study of OH vacancy in HAp [6]. This approach allows to consider also P- and OH-substitutions defects and Fe-interstitial (Fig. 3 and Fig. 4).

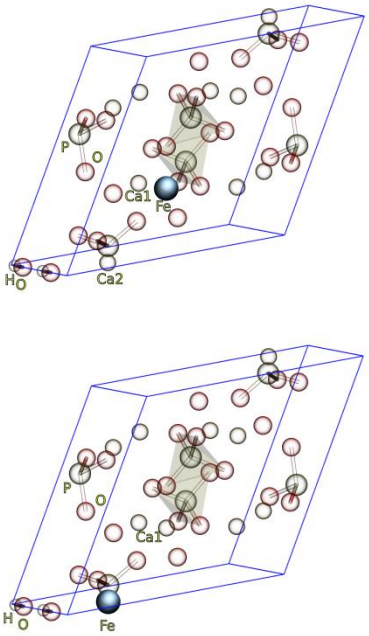

Fig. 2. Fe substitutions on calcium sites. Top – Fe on Ca(1) site (calcium column), bottom – on Ca(2) site (calcium triangle).

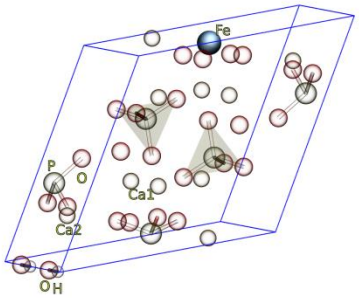

Fig. 3. Fe substitution of P (in PO_4|tetrahedra).

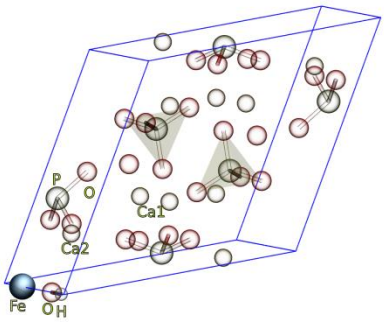

Fig. 4. Fe substitution of OH group in channel.

2.3. Iron interstitials

The iron interstitial impurities were not previously considered according to the results of X-ray diffraction (XRD) observations. However, XRD is a probe of ordered structures, and impurities are disordered by their definition. So, in current study, we have considered also three possible intersititial structure illustrated in Fig. 5.

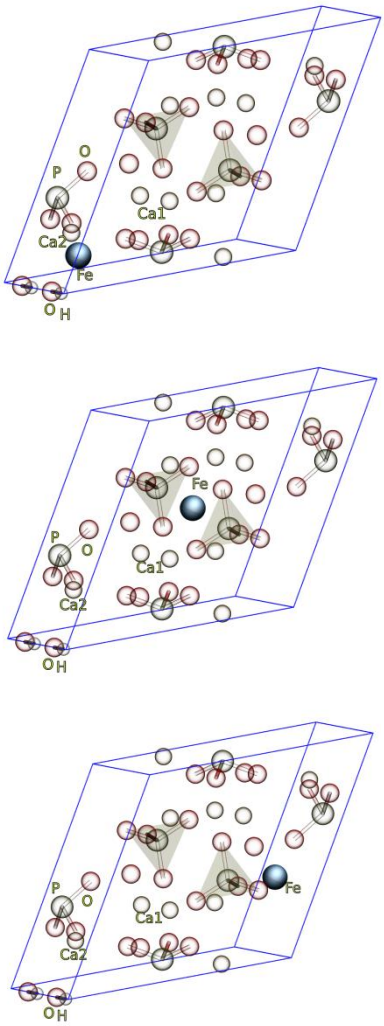

Fig. 5. Possible Fe-interstitial HAp structures: top – Fe in the center of cell, bottom – Fe in OH-channel.

3. Computational methods

The calculations were carried out using density functional theory using plane-wave wavefunction basis set, ultra-soft pseudopotentials for account of chemically inert core electrons and PBE [7] exchange-correlation functional as it implemented in Quantum Espresso code [8, 9].

Energy cutoff parameter, controlling the size of basis set, was selected at 30 Ry according to the test calculation of total energy differences between Ca(1) and Ca(2) Fe-substituted structures.

The formation energy of defect in pure HAp was calculated according:

$$E_f = E - N^{HAp}\,\mu^{HAp} - \sum \Delta n_i \mu_i + q(E_v + E_F),$$

where q is an integer referring to the charge state of the defect ($q = \Delta n_e$ is positive/negative when defect levels within the gap are depleted/filled with q electrons with respect to the neutral state). The electronic chemical potential is also conveniently expressed by invoking the Fermi energy so that $\mu_e = E_v + E_F$. The Fermi energy may vary between the valence band top (where $E_F = 0$) and conduction band bottom ($E_F = E_g$). While the first and second terms in equation can be readily obtained from a first-principles calculation, the last two terms can vary within certain limits imposed by the thermodynamic conditions. We also note that the third term only depends on defect-related species.

Table 1. Formation energies of defects

Structure	E_f, eV
Pure HAp	0
Fe→Ca(1)	7.777
Fe→Ca(2)	7.465
Fe→P	6.118
Fe→OH	10.620
Fe in cell center	6.221
Fe in OH-channel	5.657

4. Conclusions

According to calculated formation energies of defects, presented in Table 1, the following conculsons can be drown:

1) Ca(1) and Ca(2) substitutions have almost the same formation energy and equally probable.

2) the iron interstitial defects, which are not yet considered in the literature, are even more probable than substitution defects.

5. Acknowledgments

The study was supported by RFBR according to the research projects № 18-52-05004 Арм_а and 15-01-04924.

4. Reference

1. Jiang M., Terra J., Rossi A.M., Morales M.A., Baggio Saitovitch E.M., Ellis D.E. *Phys. Rev. B.* 2002. V. 66. doi: 10.1103/PhysRevB.66.224107.
2. Bystrov V. *Math. Biol. Bioinform.* 2017. V. 12. № 14.
3. Tampieri A., D'Alessandro T., Sandri M., Sprio S., Landi E., Bertinetti L., Panseri S., Pepponi Gi., Goettlicher J., Bañobre-López M., Rivas J. *Acta Biomaterialia*. 2012. V. 8. P. 843–851. doi: 10.1016/j.actbio.2011.09.032.
4. Low H.R., Phonthammachai N., Maignan A., Stewart G.A., Bastow T.J., Ma L.L., White T.J., *Inorg. Chem.* 2008. V. 47. P. 11774–11782. doi: 10.1021/ic801491t.
5. Mondal S., Manivasagan P., Bharathiraja S., Santha Moorthy M., Kim H.H., Seo H., Lee K.D., Oh J. *International Journal of Nanomedicine.* 2017. V. 12. P. 8389–8410.
6. Avakyan L.A., Paramonova E.V., Coutinho J., Öberg S., Bystrov V.S., Bugaev L.A. *The Journal of Chemical Physics*. 2018. V. 148. P. 154706. doi: 10.1063/1.5025329.
7. Perdew J.P., Burke K., Ernzerhof M. *Phys. Rev. Lett.* 1996. V. 77. P. 3865.
8. Giannozzi P., Baroni S., Bonini N., et al. *J. Phys. Condens. Matter*. 2009. V. 21. Article No. 395502. doi: 10.1088/0953-8984/21/39/395502.
9. Giannozzi P., Andreussi O., Brumme T., et al. *J. Phys. Condens. Matter*. 2017. V. 29. Article No. 465901. URL: http://iopscience.iop.org/article/10.1088/1361-648X/aa8f79 (accessed 17.08.2018).